Aerodynamic Leidenfrost effect

Anaïs Gauthier,[1,2] James C. Bird,[3] Christophe Clanet,[1,2] and David Quéré[1,2]

[1]*Physique & Mécanique des Milieux Hétérogènes, UMR No. 7636 du CNRS, ESPCI, 75005 Paris, France*
[2]*LadHyX, UMR No. 7646 du CNRS, École Polytechnique, 91128 Palaiseau, France*
[3]*Department of Mechanical Engineering, Boston University, Boston, Massachusetts 02155, USA*

When deposited on a plate moving quickly enough, any liquid can levitate as it does when it is volatile on a very hot solid (Leidenfrost effect). In the aerodynamic Leidenfrost situation, air gets inserted between the liquid and the moving solid, a situation that we analyze. We observe two types of entrainment. (i) The thickness of the air gap is found to increase with the plate speed, which is interpreted in the Landau-Levich-Derjaguin frame: Air is dynamically dragged along the surface and its thickness results from a balance between capillary and viscous effects. (ii) Air set in motion by the plate exerts a force on the levitating liquid. We discuss the magnitude of this aerodynamic force and show that it can be exploited to control the liquid and even to drive it against gravity.

I. INTRODUCTION

As described centuries ago by Boerhaave and by Leidenfrost, a volatile liquid placed on a hot solid will float on a cushion of its own vapor, provided that the solid temperature T exceeds the so-called Leidenfrost temperature T_L [1–3]. This phenomenon has unique characteristics [4]. (i) Owing to the absence of contact with the substrate, the levitating liquid is spectacularly mobile and it does not boil. (ii) The liquid presses on the underlying vapor film, causing the vapor to flow outward; balancing the vapor leak with the flux of evaporation provides the film thickness, found to be between 10 and 50 μm and to increase with temperature T. (iii) If the vapor leak is rendered directional by asymmetric textures at the solid surface, the levitating liquid can be guided by the subjacent vapor film and manipulated [5–7].

At room temperature, analogous effects can be generated in a dynamic fashion. Oil drops are observed to levitate, bounce, and even walk on the surface of a bath of the same oil, if the bath is vibrated at the right frequencies and amplitudes [8–10]. These effects are not observed with rigid substrates; yet levitation in this case can be induced by modest differences of temperature between the liquid and the solid: A hot drop on a cold surface can sit on a film of the air brought beneath the liquid by the Marangoni flow arising from the gradient of temperature [11]. A less explored situation is that of moving substrates, on which we focus in this paper. If a flat solid (or liquid) translates tangentially with enough speed, a liquid placed on it can also levitate [12–14], a phenomenon we call the aerodynamic Leidenfrost effect. We can define a Leidenfrost velocity V_L as the minimum plate speed inducing levitation; beyond V_L, the film of air carried by the plate settles between the solid and the liquid and persists in dynamic equilibrium. Thus this velocity is analogous to the Leidenfrost temperature T_L of a heated plate and it is typically 1 m/s for silicone oil. Unlike the regular Leidenfrost phenomenon, the effect can be observed with nonvolatile and viscous liquids, allowing a wide range of fluids to be rendered nonwetting, independent of the substrate wettability. As the plate velocity is increased further, even impinging drops can be repelled [15]. We discuss how the thickness h of the underlying film of air increases with the main parameter controlling levitation, namely, the plate velocity V, as it does with temperature on hot plates. In addition, air films on moving plates flow directionally and we describe how this allows us to control the motion and velocity of the levitating liquid.
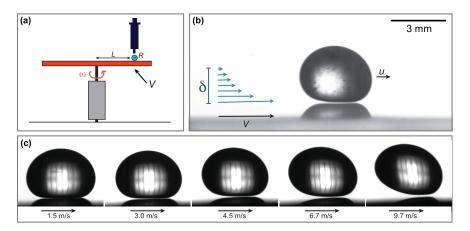
FIG. 1. Aerodynamic Leidenfrost effect. (a) Schematic of the experimental setup. A drop of viscosity $\eta = 96$ mPa s and millimeter-size radius R is gently deposited from a syringe on a disk of aluminum rotating at an angular velocity ω. The disk velocity under the drop is denoted by V. (b) Side view of a drop of silicone oil (with $R = 1.24$ mm) for $\omega = 44$ rad/s and $V = 4$ m/s (see movie 1 in Ref. [22]). Levitation is observed, as shown by the nonwetting shape of the drop and by the ray of light between the liquid and its reflection. The disk entrains a boundary layer of thickness $\delta \approx 2.5(\eta_a/\rho_a\omega)^{1/2} \approx 1.5$ mm, whose profile is sketched in blue, at the correct scale. Due to the plate motion, the drop drifts at a velocity $u \ll V$. (c) As the plate velocity V increases from 1.5 m/s to 9.7 m/s, the gap thickness also increases (see movies 2–4 in Ref. [22]). Here the drop size is kept constant with $R = 1.24$ mm.

II. EXPERIMENT

The solid substrate is a polished aluminum disk of radius 10.3 cm that is set up to rotate at an angular velocity ω between 0 and 150 rad/s [Fig. 1(a)]. Drops are deposited at a distance $L \approx 9$ cm from the plate center so that the velocity $V = L\omega$ of the surface under the drops can span from 0 to 15 m/s. As the disk spins, it entrains a laminar boundary layer of air with thickness $\delta \approx 2.5(\eta_a/\rho_a\omega)^{1/2} \approx 2.5(\eta_a L/\rho_a V)^{1/2}$, where $\eta_a = 20\,\mu$Pa s and $\rho_a = 1.2$ kg/m^3 are, respectively, the dynamic viscosity and density of air [16–19]. As V increases from 2 to 15 m/s, the thickness δ of the boundary layer decreases from 2.1 mm to 800 μm, that is, from a distance smaller than the drop diameter to a distance smaller than its radius.

We used two liquids: silicone oil, with density $\rho = 960$ kg/m^3 and surface tension $\gamma = 21$ mN/m, and a mixture of glycerol and water, with $\rho = 1225$ kg/m^3 and $\gamma = 64$ mN/m. Both liquids share a viscosity $\eta = 96$ mPa s, high enough to damp capillary waves and cause drops to keep a stationary smooth shape during levitation. Liquids are deposited from a proximal needle; their velocity at impact never exceeds 5 cm/s, which corresponds to a fall from approximately 150 μm. The drop radius R can be varied by a factor of order 2 by adjusting the size of the needles from which they are dispensed. Experiments are filmed from the side or from the top, using a high-speed camera (Optronis CR600) at typically 3000 frames/s.

Figure 1(b) shows a side view of a drop of silicone oil (radius $R = 1.24$ mm) levitating above a substrate translating at $V = 4$ m/s. Since the radius is close to the capillary length $\ell = (\gamma/\rho g)^{1/2} \approx 1.5$ mm, oil is deformed by gravity and its bottom flattened by a distance of order R. The drop is not fore-aft symmetric, but instead appears to be slightly tilted, even at small plate velocity [Fig. 1(c)]. The corresponding wedge shape of the subjacent film of air makes the drop levitate, owing to the resulting lubrication pressure [14,20,21]. Owing to backlighting, the film is visible between the drop and the reflection that the drop creates on the polished aluminum. The gap thickness h is on the order of 10 μm, which is much thinner than the millimeter-size air boundary layer. Even though the drop does not directly contact the moving substrate, its motion is influenced by the rapidly moving

air. Its drift speed u increases with time, from $u \approx 0$ when liquid is deposited to $u \approx 0.5$ m/s after it has moved a few centimeters.

Figure 1(c) shows successive shapes adopted by drops with increasing substrate velocity V. We report changes as the plate gets faster. (i) The air film thickens with increasing velocity. The ray of light beneath the liquid, almost invisible for $V = 1.5$ m/s, reaches a thickness h close to 100 μm for $V = 9.7$ m/s. Movies indicate that the drift speed u also increases with V (see [22]). (ii) Above a velocity of approximately 7 m/s, the liquid is so deformed by the air that the flat region under the drop shrinks. We focus here on two main characteristics of the aerodynamic Leidenfrost effect: the thickness h of the air film, and the origin and intensity of the drift arising from aerodynamics.

III. HEIGHT OF LEVITATION

Various techniques have been used in the past to measure the film thickness beneath levitating liquids, such as diffraction [23] or colored interferences for micrometric films [14,24]. These techniques cannot be used in our experiment for two reasons. First, the levitating drops are mobile and remain in the field of view for less than 1 s. Second, the air gap in our experiments is between 10 and 100 μm, which is too thick to generate exploitable colored interferences. Instead, the film thickness is directly extracted from the backlit, high-speed images [Figs. 1(b) and 1(c)]. For each of these images, we identify the location of the smallest air gap [Fig. 2(a), framed in blue]. The drop and its reflection on aluminum form two dark regions separated by a lighter zone of thickness $2h$; the mirror effect plays the role of a zoom. In this area of $200 \times 150 \, \mu m^2$, we measure (using the software MATLAB) the gray shade of each pixel i along the vertical axis z. The scale varies from to 0 (black) to 255 (white) and $z = 0$ defines the center of the light zone. By comparing i to the darkest shade i_0, we deduce the relative intensity $I = (i - i_0)/255$ of each pixel. Figure 2(b) shows how I varies as a function of z, for different plate velocities V and silicone oil drops of radius $R = 1.24$ mm. All data are convincingly fitted by a Gaussian curve, whose height and width increase with V. The thickness h of the air film is finally deduced from the width of these curves.

Figure 2(c) shows how the air gap thickness h varies with the surface velocity V. Here smaller drops ($R = 1.24$ mm) of silicone oil (black data points) and glycerol (blue data points) are plotted alongside larger ($R = 1.68$ mm) drops of glycerol (red data points). For silicone oil, V is varied between 0.8 and 6.7 m/s; below $V = 0.8$ m/s, drops contact the surface and above $V = 6.7$ m/s, they become noticeably tilted and are beyond the scope of this study [Fig. 1(c)]. For glycerol, the range of explored velocities is slightly smaller because the air film is not visible for $V < 6$ m/s.

Figure 2(c) shows that the gap thickness h increases with the plate velocity V, confirming the observations made in Fig. 1(c). For silicone oil, h varies from 8 to 28 μm as V rises from 0.8 to 6.7 m/s; dynamical Leidenfrost gaps are slightly thinner than typical vapor gaps on hot plates. Comparing the two series of liquids at fixed size ($R \approx 1.24$ mm) and speed ($V \approx 7$ m/s) indicates that h decreases from $27 \pm 5 \, \mu$m for oil to $14 \pm 2 \, \mu$m for glycerol (whose surface tension is 3 times larger), a thinning of almost 50%. Observations at small velocity agree with that by Lhuissier *et al.* obtained by colored interferometry [14] [open symbols in Fig. 2(c)]. In addition, we observe that big drops levitate higher than small ones; h is systematically larger (by about 25%) for $R = 1.68$ mm (red data) than for $R = 1.24$ mm (blue data).

We interpret these results by recognizing a connection to the Landau-Levich-Derjaguin (LLD) problem [25,26]; specifically, a plate drawn out of a bath will be coated with a film of a particular thickness. In our study, a plate moves and entrains a film (of air) in an atmosphere made of a viscous liquid, a situation leading to the same scaling law as in the original LLD situation [27]. In both cases, the key dynamical parameter is the capillary number that compares viscous effects (favoring entrainment) and capillary action (opposing it). In the aerodynamic Leidenfrost case, the velocity of the plate is large (a few m/s), but the viscosity of the entrained phase is low ($\eta_a = 20 \, \mu$Pa s). Thus the capillary number $Ca = \eta_a V / \gamma$ is typically of order 10^{-3}, fully in the domain of validity of the LLD model. The distance normalizing the thickness h is the static size of the meniscus joining the reservoir to the film, a role played here by the drop radius R [28]. Hence we expect the air thickness
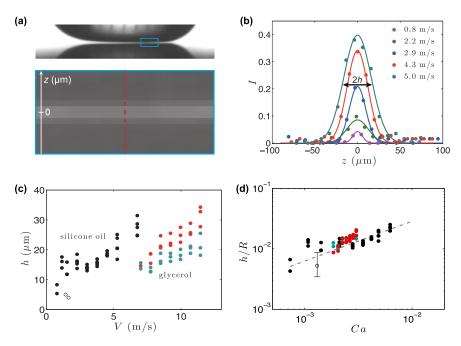
FIG. 2. Measurements of air gap thickness. (a) Base of a drop of silicone oil ($R = 1.24$ mm) levitating above an aluminum plate moving from left to right at $V = 3.0$ m/s. The thickness of air is measured in the flat zone where it is minimum (blue box). In this area, the gray shade of each pixel is measured along the dashed vertical line as a function of the position z. (b) Variations of the pixel intensity I as a function of z, for five surface velocities V. Circles show data and lines are Gaussian fits, whose width provides the thickness h. (c) Air thickness h as a function of plate velocity V. Black and blue data points correspond to silicone oil and glycerol of radius $R = 1.24$ mm and red data points correspond to bigger drops of glycerol ($R = 1.68$ mm). Open symbols indicate measurements by Lhuissier *et al.* [14], performed by colored interferometry through a transparent substrate (for $R = 1.16$ and 1.39 mm). (d) A log-log plot of the ratio h/R as a function of the capillary number $\mathrm{Ca} = \eta_a V/\gamma$, with η_a the air viscosity and γ the surface tension of the drop. The open symbol summarizes all the data by Lhuissier *et al.* [14], obtained at a velocity $V = 1.54 \pm 0.11$ m/s and $R = 0.55$, 1.16, and 1.39 mm. The data collapse and they are consistent with the power law $h = 0.60R\,\mathrm{Ca}^{2/3}$ represented by a dotted line.

to scale as

$$h \sim R(\eta_a V/\gamma)^{2/3}. \tag{1}$$

We plot the data of Fig. 2(c) in the log-log scales of Fig. 2(d), as a function of the capillary number $\mathrm{Ca} = \eta_a V/\gamma$ relating to air entrainment. Our interpretation in the LLD framework is first supported by the collapse of the data. The slope $2/3$ suggested by Eq. (1) is drawn with a dashed line, with fair agreement with the data (on a limited scale, however). Importantly, Eq. (1) predicts correct orders of magnitude for the observed thicknesses, since the fit in Fig. 2(d) is obtained with a coefficient of 0.60 ± 0.20, of order unity as expected in this framework [25–28], even if this value remains to be understood.

It is worth discussing limitations of the model. First, the viscous boundary layer must be thick enough to consider viscous entrainment. This condition can be expressed as $\delta > h$, which is well satisfied in our experiments. Indeed, for δ to become of the size as h would require V to be of order 100 m/s, far beyond the velocities in this study. Second, inertia of the entrained fluid must remain negligible compared to capillary action, a condition for applying LLD analysis, where inertial effects are ignored. This condition can be written $\rho_a V^2 < \gamma/R$, which implies $V < (\gamma/\rho_a R)^{1/2}$. The
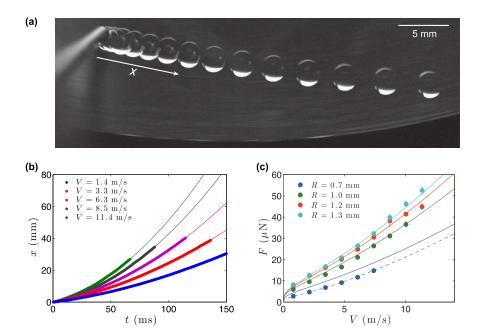
FIG. 3. Estimating aerodynamic forces from drop acceleration. (a) Chronophotograph of a drop of silicone oil ($R = 1.25$ cm) deposited at 1 cm from the edge of a plate rotating at $V = 3.5$ m/s. Successive images are separated by 12.5 ms. The drop is entrained along a quasistraight line and its position is denoted by x. (See movies 5 and 6 in Ref. [22].) (b) Position x as a function of time t for various plate velocities V. Thin lines are parabolic fits $x = at^2$, from which we deduce a constant force of entrainment $F = 2ma$. (c) Force F as a function of plate velocity V, for various drop radii R. Lines show Eq. (2) drawn with $\alpha = 3$ and $\beta = 0.55$. The dotted line is the best fit ($\alpha = 1.7$ and $\beta = 0.55$) for the smallest droplet of radius $R = 0.7$ mm.

plate velocity must be smaller than typically 5 m/s for oil and 8 m/s for glycerol. The high-speed limit $V > (\gamma/\rho_a R)^{1/2}$ also expresses the condition for having a drop perturbed by air at the scale δ, $\rho_a V^2 R\delta > \gamma\delta$, as indeed observed in the last snapshot of Fig. 1(c). This necessarily affects the LLD law, as a cornerstone of the law is a matching of the film profile with a quasistatic meniscus. This high-speed regime is not considered in Fig. 2, our study focusing on the purely viscous regime of air entrainment for which the liquid drop keeps a quasistatic shape [four first pictures in Fig. 1(c)].

IV. DROP ENTRAINMENT

A drop levitating above a moving plate does not stay motionless. As illustrated in the chronophotograph in Fig. 3(a) (where images are separated by even time intervals $\tau = 12.5$ ms), the liquid (here silicone oil with $R = 1.25$ mm) drifts along a nearly straight line towards the edge of the plate. The distance between successive images increases, which indicates that the drop accelerates; the drift velocity begins at $u \approx 0$ when it is deposited and has increased to $u = 0.35$ m/s when the drop reaches the edge of the disk. Note that the velocity u always remains much smaller than V, here equal to 3.5 m/s.

To characterize the aerodynamic force acting on the liquid, we follow the successive positions $x(t)$ of the drop center along its trajectory. The origin $x = 0$ is taken at the vertical of the needle [visible on the left in Fig. 3(a)]. Figure 3(b) shows $x(t)$ for silicone oil ($R = 1.25$ mm) at various plate velocities V. In each case, $x(t)$ increases as t^2, as shown by the parabolic fits (thin lines), which suggests that the liquid is uniformly accelerated by a constant force F. We can deduce the force F from the trajectory $x(t) = (F/2m)t^2$ and we report in Fig. 3(c) its value as a function of V for four

drop radii. The entrainment force is on the order of $10\,\mu$N and increases with the plate velocity V. The variation looks close to linear; similar observations with glycerol are given in Ref. [22]. As seen in Fig. 3(a), the radial distance L can vary by about 5% along the trajectory, which impacts V and thus F by the same amount; this small correction is not observable in Fig. 3(b). We also notice that the force F is more intense for bigger drops: At $V = 5\,$m/s, for instance, F is two times larger for $R = 1.3\,$mm than for $R = 0.7\,$mm.

Because the force F appears to increase somewhat linearly with V and R, one might naively postulate a Stokes law of the form $F \sim \eta_a R V$, with η_a denoting the viscosity of air. However, such a force is typically $0.1\,\mu$N for millimeter-size drops in air flowing at $V = 10\,$m/s, which is 100 times smaller than experienced by the liquid. In order to understand the underlying nature of entrainment, we need to carefully determine how drops interact with the boundary layer of air. Given that the boundary layer moves faster than the drop, the air must go either around or below the liquid. The Reynolds numbers associated with these two flows are markedly different. In the first case, air is deflected at the drop scale, so the Reynolds number can be expressed as $\text{Re} = \rho_a R V / \eta_a$, which is a quantity of order 1000 for $R = 1\,$mm and $V = 10\,$m/s. At such high values, we expect this air to exert an inertial force F_i on the liquid. The force scales as the product of the dynamical pressure $\rho_a V^2$ and the cross-sectional area $R\delta$ of the drop subjected to airflow, since we have $\delta < R$ in situations considered here. Hence we find that the force $F_i \sim \rho_a V^2 R\delta \sim (\eta_a \rho_a L)^{1/2} R V^{3/2}$ scales linearly in R and increases as $V^{3/2}$. For a millimeter-size drop and $V \approx 10\,$m/s (to which $d \approx 1.0\,$mm corresponds), we predict that air will exert an inertial force on the liquid of order $100\,\mu$N, as indeed reported in Fig. 3(c). In the second case, air is sheared under the drop, so the Reynolds number relating to air motion in the gap of thickness h is $\text{Re} = \rho_a V h^2 / \eta_a R$, of order 0.1 for $R = 1\,$mm and $V = 10\,$m/s. Air moving beneath the drop exerts on it a viscous drag F_v scaling as $(\eta_a V / h) R^2$, where the viscous stress $\eta_a V / h$ is integrated over the surface area of the drop base, a quantity scaling as R^2 for big drops. Using Eq. (1), we deduce that this force $F_v \sim (\eta_a \gamma^2)^{1/3} R V^{1/3}$ also scales linearly with R and increases as $V^{1/3}$. For $V = 1\,$m/s (and $h \approx 6\,\mu$m), F_v is expected to be a few μN, in agreement with the data in Fig. 3(c).

The forces F_i and F_v both act on the drop with comparable amplitudes for $1\,$m/s $< V < 10\,$m/s, even if the inertial force eventually prevails at higher velocity. Adding them, we get

$$F \approx \alpha(\eta_a \gamma^2)^{1/3} R V^{1/3} + \beta(\eta_a \rho_a L)^{1/2} R V^{3/2}, \tag{2}$$

where α and β are numerical coefficients. The force estimated by Eq. (2) is plotted using a solid line in Fig. 3(c) with $\alpha = 3.0$ and $\beta = 0.55$, two values found to provide excellent agreement with the data. The apparent linearity of $F(V)$ thus appears to be well described by the sum of two functions varying as $V^{1/3}$ and $V^{3/2}$. However, the friction on the smallest drop ($R = 0.7\,$mm, blue circles) is overestimated by the model (blue line). This slight discrepancy is consistent with our arguments: Nonwetting drops significantly smaller than the capillary length ℓ are quasispherical and their base reduces to R^2 / ℓ, instead of R for larger drops [29]. This geometrical effect lowers the viscous force experienced by the drop. Dividing the coefficient α by a factor of order 2 (keeping β unchanged) yields an excellent fit [dashed line in Fig. 3(c)] with the data. Note finally that using glycerol instead of silicone oil also leads to good agreement between data and Eq. (2), as shown in Ref. [22].

The force F measured and calculated is typically $10\,\mu$N, that is, comparable to the weight of millimeter-size droplets. This suggests that drops on an inclined moving plate could have the ability to climb against gravity. This experiment can be performed with our device, by tilting the rotating disk by an angle θ. We present in Fig. 4 a chronophotograph showing a drop of silicone oil (with $R = 0.94\,$mm) placed on a plate tilted by $\theta = 22°$ and moving upward at $V = 9\,$m/s. It is observed that the force F is indeed high enough to overcome gravity, so the levitating liquid accelerates along the slope.

Hence it is possible to control the movement of levitating drops by modifying the substrate velocity V. One can choose to make drops go up or down on inclines or even to maintain them on the same spot for a long time, as shown in movies 7–9 in Ref. [22]. We also imagine using this
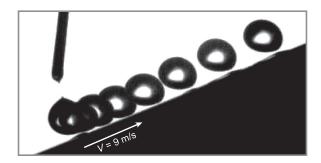
FIG. 4. Chronophotograph of a drop of silicone oil ($R = 0.94$ mm) dispensed by a needle (on the left) on a surface inclined by an angle of $22°$ and moving to the right at $V = 9$ m/s. The aerodynamic entrainment force F is large enough to push oil up and accelerate it against gravity. Successive images are separated by 8 ms.

phenomenon to select droplets of different sizes: F increases linearly with R, which means that for a given surface velocity V, small drops can climb while big ones will run down.

V. CONCLUSION

We discussed in this paper two kinds of entrainment observed as a liquid is brought in contact with a moving plate. (i) Air is entrained by the plate, which generates the levitation of the liquid (aerodynamic Leidenfrost effect); the thickness of the air gap separating the liquid from its substrate is itself a dynamical quantity found to increase with the plate velocity, in agreement with the Landau-Levich-Derjaguin law. (ii) Despite the absence of solid-liquid contact, the liquid drifts tangentially at a velocity that increases with the plate speed. We find that this drag is viscoinertial, as the drop is both inertially pushed by the deflected air around the drop and viscously dragged by the film below it. As a consequence, the aerodynamic Leidenfrost phenomenon not only induces liquid repellency, but also allows us to control the resulting elusive drops by adjusting the velocity of their substrate. Additionally, the phenomenon can significantly reduce heat transfer (as it does in classical Leidenfrost effect), which might affect the efficacy of the spray cooling of rapidly translating or rotating equipment.

Many questions remain. It would be interesting to look at much smaller drops, for which the condition $\delta < R$ is not satisfied anymore. We expect such drops to be quasispherical, which should modify the underlying flow of air; being fully embedded in the viscous boundary layer, these droplets might be driven much quicker, at a velocity closer to the plate speed V, unlike larger volumes of liquid. Another interesting (and opposite) limit is that of very fast plate motion, for which turbulence in the air layer should perturb our results; even without turbulence, fast motions lead to strong deformation of the liquid profile [as observed in Figs. 1(c) and 4 and discussed above], a regime that also remains to be fully characterized.

ACKNOWLEDGMENT

[1] H. Boerhaave, *Elementa Chemiae* (Lugduni Batavorum, Leiden, 1732).

[2] J. G. Leidenfrost, *Impensis Hermanni Ovenni* (Universität Bibliopolæ, Duisbourg, 1756).

[3] J. D. Bernardin and I. Mudawar, The Leidenfrost point: Experimental study and assessment of existing models, J. Heat Transfer **121**, 894 (1999).

[4] D. Quéré, Leidenfrost dynamics, Annu. Rev. Fluid Mech. **45**, 197 (2013).

[5] H. Linke, B. J. Alemán, L. D. Melling, M. J. Taormina, M. J. Francis, C. C. Dow-Hygelund, V. Narayanan, R. P. Taylor, and A. Stout, Self-Propelled Leidenfrost Droplets, Phys. Rev. Lett. **96**, 154502 (2006).

[6] G. Dupeux *et al.*, Viscous mechanism for Leidenfrost propulsion on a ratchet, Europhys. Lett. **96**, 58001 (2011).

[7] T. R. Cousins, R. E. Goldstein, J. W. Jaworski, and A. I. Pesci, A ratchet trap for Leidenfrost drops, J. Fluid Mech. **696**, 215 (2012).

[8] Y. Couder, E. Fort, C.-H. Gautier, and A. Boudaoud, From Bouncing to Floating: Noncoalescence of Drops on a Fluid Bath, Phys. Rev. Lett. **94**, 177801 (2005).

[9] Y. Couder, S. Protière, E. Fort, and A. Boudaoud, Dynamical phenomena: Walking and orbiting droplets, Nature (London) **437**, 208 (2005).

[10] J. Bush, Pilot-wave hydrodynamics, Annu. Rev. Fluid Mech. **47**, 269 (2015).

[11] P. T. Nagy and G. P. Neitzel, Optical levitation and transport of microdroplets: Proof of concept, Phys. Fluids **20**, 101703 (2008).

[12] K. R. Sreenivas, P. K. De, and J. H. Arakeri, Levitation of a drop over a film flow, J. Fluid Mech. **380**, 297 (1999).

[13] A. Duchesne, C. Savaro, L. Lebon, C. Pirat, and L. Limat, Multiple rotations of a drop rolling inside a horizontal circular hydraulic jump, Europhys. Lett. **102**, 64001 (2013).

[14] H. Lhuissier, Y. Tagawa, Y. Tran, and C. Sun, Levitation of a drop over a moving surface, J. Fluid Mech. **733**, R4 (2013).

[15] O. A. Povarov, O. I. Nazarov, L. A. Ignat'evskaya, and A. I. Nikol'skii, Interaction of drops with boundary layer on rotating surface, J. Eng. Phys. Thermophys. **31**, 1453 (1976).

[16] T. von Kármán, Über laminare und turbulente reibung, Z. Angew. Math. Mech. **1**, 233 (1921).

[17] N. Gregory, J. T. Stuart, and W. S. Walker, On the stability of three-dimensional boundary layers with application to the flow due to a rotating disk, Philos. Trans. R. Soc. London Ser. A **248**, 155 (1955).

[18] R. J. Lingwood, An experimental study of absolute instability of the rotating-disk boundary-layer flow, J. Fluid Mech. **314**, 373 (1996).

[19] M. E. Siddiqui, V. Mukund, J. Scott, and B. Pier, Experimental characterization of transition region in rotating-disk boundary layer, Phys. Fluids **25**, 034102 (2013).

[20] D. Dowson and C. M. Taylor, Cavitation in bearings, Annu. Rev. Fluid Mech. **11**, 35 (1979).

[21] J. Ashmore, C. Del Pino, and T. Mullin, Cavitation in a Lubrication Flow Between a Moving Sphere and a Boundary, Phys. Rev. Lett. **94**, 124501 (2005).

[22] See Supplemental Material at http://link.aps.org/supplemental/10.1103/PhysRevFluids.1.084002 for supplementary figure and movies.

[23] A. L. Biance, C. Clanet, and D. Quéré, Leidenfrost drops, Phys. Fluids **15**, 1632 (2003).

[24] R. C. van der Veen, T. Tran, D. Lohse, and C. Sun, Direct measurements of air layer profiles under impacting droplets using high-speed color interferometry, Phys. Rev. E **85**, 026315 (2012).

[25] L. Landau and B. Levich, Dragging of a liquid by a moving plate, Acta Physicochim. (USSR) **17**, 42 (1942).

[26] B. Derjaguin, Thickness of liquid layer adhering to walls of vessels on their emptying and the theory of photo- and motion-picture film coating, C. R. (Dokl.) Acad. Sci. URSS **39**, 13 (1943).

[27] L. W. Schwartz, H. M. Princen, and A. D. Kiss, On the motion of bubbles in capillary tubes, J. Fluid Mech. **172**, 259 (1986).

[28] F. P. Bretherton, The motion of long bubbles in tubes, J. Fluid Mech. **10**, 166 (1961).

[29] L. Mahadevan and Y. Pomeau, Rolling droplets, Phys. Fluids **11**, 2449 (1999).